Cold Atom Clocks

Y. Sortais[†], S. Bize[†], M. Abgrall[†], S. Zhang[†], C. Nicolas[†], C. Mandache[†]
P. Lemonde[†], P. Laurent[†], G. Santarelli[†], N. Dimarcq[††], P. Petit[††], A. Clairon[†]
A. Mann[†††], A. Luiten[†††], S. Chang[†††]
C. Salomon[*]

[†]BNM-LPTF, Observatoire de Paris, 61 Av. de l'Observatoire, 75014, Paris, France
E-mail : yvan.sortais@obspm.fr
[††] Laboratoire de l'Horloge Atomique, bat. 221, Université Paris sud, 91405 Orsay, France.
[†††] Physics Department, University of Western Australia, Nedlands, 6907 WA, Australia.
[*]Laboratoire Kastler Brossel, Ecole Normale Supérieure, 24 rue Lhomond,
75231, Paris, France.

PACS Ref : 06.30.Ft, 32.80.Pj, 34.20.Cf

Abstract

This paper reviews recent progress on microwave clocks using laser cooled neutral atoms. With an ultra-stable cryogenic sapphire oscillator as interrogation oscillator, a cesium fountain operates at the quantum projection noise limit. With 6 10^5 detected atoms, the relative frequency stability $\delta\nu/\nu$ is 4 10^{-14} $\tau^{-1/2}$ where τ is the integration time in seconds. This stability is comparable to that of hydrogen masers. At $\tau = 2$ 10^4 s, the measured stability reaches 6 10^{-16}. Equally important is the accuracy of the frequency standard since ^{133}Cs is the primary reference for the definition of the time unit, the second. The accuracy of our cesium fountain FO1 is presently 1 10^{-15}, currently the best reported value.

A ^{87}Rb fountain has also been constructed and the ^{87}Rb ground-state hyperfine energy has been compared to the Cs primary standard with a relative accuracy of 2.5 10^{-15}. Comparing the hyperfine energies of atoms with different atomic numbers Z, one can search for possible variations of the fine structure constant $\alpha = e^2/\hbar c$ with time. Measurements of the ratio $\nu(^{87}Rb)/\nu(^{133}Cs)$ spread over an interval of 24 months indicate no change at a level of 3.1 10^{-15}/year, placing a new upper limit for $1/\alpha(d\alpha/dt)$. The second attractive feature of ^{87}Rb fountains is the smallness of the frequency shift induced by the mean field interaction between atoms. This shift is found to be at least ~ 50 times below that of cesium.

Finally, the interest of the microgravity of space for cold atom experiments is outlined. A space mission, ACES, carrying ultra-stable clocks, is presented. ACES has been selected by the European Space Agency to fly on the International Space Station in 2004.

1 INTRODUCTION

Since 1967, the SI unit of time, the second, is based on a quantum oscillator using the ground-state hyperfine transition in atomic ^{133}Cs. By definition, the frequency of this transition is 9 192 631 770 Hz. The best realization of the second is currently achieved by laser cooled ^{133}Cs atomic fountains which combine both high stability and high accuracy. The evolution of the relative accuracy of ^{133}Cs primary frequency standards with time is shown in fig.1. Since the 1960's, it has improved on average by a factor of 10 every 10 years, reaching currently 10^{-15} in cold atom fountains. For comparison the microwave trapped ion frequency standard based on Hg^+ [2] and the recent optical measurements of the 1s-2s transition in atomic hydrogen [3] and of the 657 nm transition in calcium [4] are also shown in fig.1.

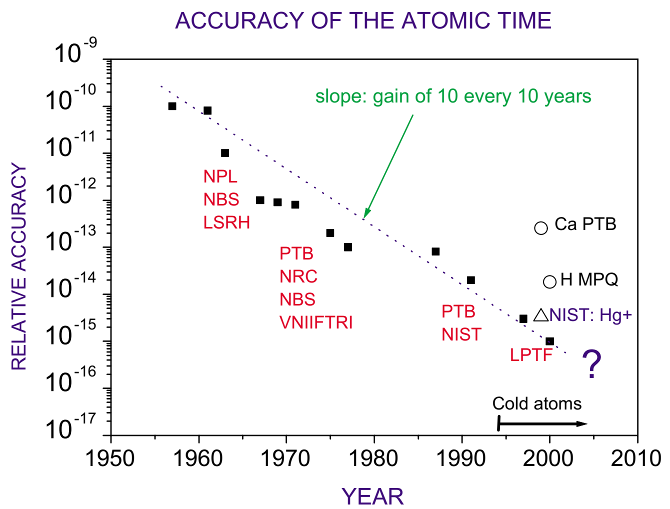

Figure 1: Accuracy of cesium atomic clocks over the last 40 years (black squares). Open triangle: Hg^+ ion at 40 GHz [2]. Open circles : H [3] and Ca [4] optical lines.

In passive atomic clocks, the relative frequency stability

$\sigma_y(\tau)$ is given by the Allan variance of the frequency fluctuations of a macroscopic oscillator (a quartz crystal, or a sapphire cryogenic oscillator), slaved to the resonance of a sample of microscopic oscillators (Cs atoms in a primary standard). Here, τ is the measurement time. This Allan variance is always measured using the beat note between two independent oscillators. The accuracy of an atomic clock depends on various parameters such as the temperature of the experiment, the surrounding magnetic field, or the collisions between the atoms.

Cold atom clocks use the method of separated oscillatory fields introduced by Ramsey in 1950, but adapted to a vertical geometry [5, 6]. The atoms are first prepared in one of the two levels $|g\rangle$ and $|e\rangle$ of the clock transition, and then launched upwards. On the way up, they pass through a resonant microwave cavity. The microwave frequency is generated from the macroscopic oscillator and tuned to the clock transition. The atoms interact with the microwave field sustained inside the cavity, and undergo a first $\pi/2$ pulse. On the way down, they pass through the same cavity, where they undergo after a time T a second $\pi/2$ pulse. The longer T, the narrower the Ramsey resonance, and the higher the frequency resolution. After the Ramsey interactions, the populations N_g and N_e of both clock levels are measured. From the transition probability signal, $N_e/(N_g + N_e)$, as a function of the microwave detuning, an error signal is computed to lock the macroscopic oscillator to the atomic transition. In fig.2, the Ramsey resonance as a function of the microwave frequency is shown for the BNM-LPTF Cs fountain FO1. The atoms are cooled down to 0.8 μK and launched upwards at $\sim 4\,\mathrm{m/s}$. They reach apogee $\sim 30\,\mathrm{cm}$ above the microwave cavity, corresponding to $T \sim 0.5\,\mathrm{s}$. Ramsey fringes have a width $\Delta\nu = 1\,\mathrm{Hz}$ FWHM. Each point is one cycle of duration 1.1 s, and the signal to noise ratio is 2000 for 8 10^5 detected atoms.

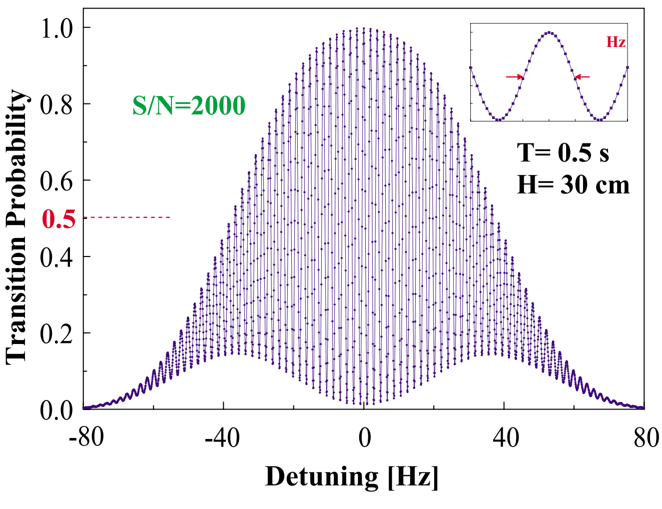

Figure 2: Ramsey fringes of the BNM-LPTF Cs fountain FO1. The fringe width is 1 Hz and signal to noise ratio is 2000 per cycle of 1.1 s.

In this paper, we discuss the present performance and limits of ^{133}Cs and ^{87}Rb fountains. We have recently shown that Cs fountains can be operated with a frequency stability limited by the quantum projection noise [7]. The accuracy of BNM-LPTF CS fountains has been improved up to 1.0 10^{-15}. Going much beyond seems a hard task, because of the large frequency shift induced by cold collisions. In contrast, ^{87}Rb fountains exhibit a collisional shift ~ 50 times smaller than in ^{133}Cs [8, 9]. ^{87}Rb fountains are thus interesting candidates for future atomic clocks with better performance. We present the measurement of the collisional shift in our ^{87}Rb fountain and we give a new limit for the variation of the fine structure constant $\alpha = e^2/\hbar c$ with time. Finally, micro-gravity environment is capable of providing even longer interaction times than in Earth fountains [10, 11].

2 Cs FOUNTAINS

Until recently, the frequency stability of atomic fountains was limited by the phase noise of the quartz oscillator used for the atom interrogation. With state-of-the-art quartz oscillators, this limit is above $10^{-13}\,\tau^{-1/2}$ [12]. With such a stability, a 10^{-16} accuracy goal is challenging since a single measurement with this resolution implies an averaging time of more than one week. By using an ultra-stable cryogenic sapphire oscillator (SCO) developed by the University of Western Australia [13], we have been able to overcome this limitation and to reach the quantum projection noise limit [7, 14, 15].

Before being detected, the atomic internal state is a linear superposition of the two states $|e\rangle$ and $|g\rangle$ of the clock transition: $|\psi\rangle = \alpha|g\rangle + \beta|e\rangle$, with $|\alpha|^2 + |\beta|^2 = 1$. The measurement process projects atoms in state $|e\rangle$ or $|g\rangle$. The probability of finding an atom in $|e\rangle$ is $|\beta|^2 = \langle\psi|P_e|\psi\rangle = p$, with P_e the projection operator onto state $|e\rangle$. The measurement exhibits quantum fluctuations of standard deviation $\sigma = \left(\langle\psi|P_e^2|\psi\rangle - (\langle\psi|P_e|\psi\rangle)^2\right)^{1/2} = \sqrt{p(1-p)}$. For a set of N_{at} uncorrelated atoms, σ scales as $N_{at}^{-1/2}$. Itano *et. al.* [15] named this effect *quantum projection noise* and have observed it both in the case of repeated measurements on a single particle prepared successively under identical conditions, and in the case of an ensemble average with a number N_{at} of identical trapped particles, up to $N_{at} = 380$.

The SCO possesses a mode which is only 1.3 MHz away from the Cs hyperfine splitting frequency ν_0. Oscillating on this mode, its frequency stability is below 10^{-14} from 0.1 to 10 s. The excess noise is then negligible compared to the projection noise in our atomic fountain for $N_{at} \leq 10^6$. The Allan standard deviation of the relative frequency fluctuations $y(t)$ of an atomic fountain can be expressed as:

$$\sigma_y(\tau) = \frac{1}{\pi Q_{at}}\sqrt{\frac{T_c}{\tau}}\left(\frac{1}{N_{at}} + \frac{1}{N_{at}n_{ph}} + \frac{2\sigma_{\delta N}^2}{N_{at}^2} + \gamma\right)^{1/2} \tag{1}$$

In (1) τ is the measurement time in seconds, T_c is the fountain cycle duration ($\sim 1\,\mathrm{s}$) and $\tau > T_c$. $Q_{at} = \nu_0/\Delta\nu$

is the atomic quality factor. The first term in parentheses is the atomic projection noise $\propto N_{at}^{-1/2}$. The second term is due to the photon shot-noise of the detection fluorescence pulses and is less than 1% of the projection noise. The third term represents the effect of the noise of the detection system. $\sigma_{\delta N}$, the uncorrelated rms fluctuations of the atom number per detection channel, is about 85 atoms per fountain cycle. This noise contribution becomes less than the projection noise when $N_{at} > 2\ 10^4$. γ is the contribution of the frequency noise of the interrogation oscillator [16, 12]. With the SCO, this contribution is at most $10^{-14}\tau^{-1/2}$ and can be neglected. As an example, for $N_{at} \sim 6\ 10^5$ detected atoms, $\Delta\nu = 0.8\,\text{Hz}$, $Q_{at} = 1.15\ 10^{10}$ and $T_c = 1.1\,\text{s}$, the expected frequency stability is $\sigma_y(\tau) = 4\ 10^{-14}\tau^{-1/2}$.

To observe the quantum projection noise, we vary the number of atoms in the fountain and measure the frequency stability $\sigma_y(\tau)$ by comparison with the free running sapphire oscillator which is used as a very stable reference up to $10-20$ seconds. A plot of the normalized Allan standard deviation as a function of atom number is presented in fig.3. Since we explored several values of Q_{at} and of the cycle duration T_c, we plot the quantity $\sigma_y(\tau)\pi Q_{at}\sqrt{\tau/T_c}$ for $\tau = 4\,\text{s}$. This quantity should simply be equal to $N_{at}^{-1/2}$ when the detection noise is negligible. At low atom numbers, the $1/N_{at}$ slope indicates that the stability is limited by the noise of the detection system (third term in eq. 1). For $N_{at} > 4\ 10^4$, the experimental points are in good agreement with the relation $y = aN_{at}^{-1/2}$ with $a = 0.91(0.1)$, close to the expected value of 1 (fig.3).

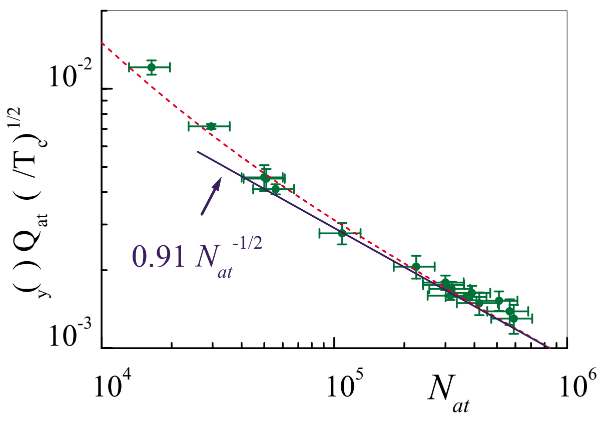

Figure 3: Normalized frequency fluctuations as a function of the number of detected atoms N_{at}. The expected quantum projection noise law is $y = N_{at}^{-1/2}$. The thick line $y = 0.91(0.1)N_{at}^{-1/2}$ is a least square fit to the experimental points for $N_{at} > 4\ 10^4$. The dashed line is the quadratic sum of the detection noise and quantum projection noise.

With the largest number of detected atoms, $N_{at} = 6\ 10^5$, the stability is $4\ 10^{-14}\tau^{-1/2}$ for $Q_{at} = 1.15\ 10^{10}$, $T_c = 1.1\,\text{s}$. This is a significant improvement over the fountain operation with a quartz oscillator. It is comparable to the best short-term stability achieved with microwave ion clocks using uncooled $^{199}Hg^+$ and $^{171}Yb^+$ samples [17, 18]. In a second experiment, we have locked the SCO to the fountain signal for $N_{at} = 5\ 10^5$ and compared it to a hydrogen maser. The Allan standard deviation of this frequency comparison is $7\ 10^{-14}\tau^{-1/2}$ and reaches $6\ 10^{-16}$ at $\tau \sim 2\ 10^4\,\text{s}$, a value close to the flicker floor of the H-maser.

Table 1: Present accuracy budget of the ^{133}Cs fountain FO1. The device operates with a stability of $1.5\ 10^{-13}\tau^{-1/2}$, and a number of detected atoms of 10^5. The MOT is disabled and atoms are captured in optical molasses. The temperature is 0.8 μK. The gravitational redshift is not intrinsic to the clock and is not included in the table.

Effect	Correction $[10^{-15}]$	Uncertainty $[10^{-15}]$
2^{nd} order Zeeman shift	-133	$\leq$ 0.1
Blackbody radiation	+17.6	$\leq$ 0.3
Microwave spectrum	0	0.2
First Order Doppler	0	$\leq$ 0.5
Microwave leaks	0	0.2
Pulling by other lines	0	0.4
Second order Doppler and gravitation	0	<< 0.1
Microwave photon	-0.3	0.3
Cold collisions + Cavity Pulling (Molasses)	1	$\leq$ 0.5
Background gas collisions	0	$\leq$ 0.5
Total 1σ uncertainty		$1.0\ 10^{-15}$

Table 1 presents the current accuracy budget of the Cs fountain FO1. The accuracy evaluation was performed by amplifying the systematic effects when possible as described in [19] and with a resolution for each measurement of 10^{-15}. This fountain has the best accuracy ever reported for frequency standards. This accuracy is currently a factor of three better than the trapped Hg^+ ion frequency standard operating at 40 GHz [2].

In the near future, direct comparison of our Cs fountains should lead to a stability on the order of $\sqrt{2} \times 4 \times 10^{-14}\tau^{-1/2}$, reaching 2×10^{-16} for $\tau \simeq 1\,\text{day}$. However under these conditions, the collisional frequency shift of the Cs clock transition is on the order of -5×10^{-15}. Reaching the 10^{-16} level of accuracy requires a stability of the average atomic density and an extrapolation to zero density at the 2% level, a delicate task.

3 ^{87}Rb : AN INTERESTING ALKALI

In 1997, Kokkelmans *et al.* predicted that the collisional frequency shift for ^{87}Rb was 15 times smaller than for

^{133}Cs [20]. Rubidium fountains could then operate with larger atom numbers, with a better short term stability and better accuracy. ^{87}Rb fountains appear thus as an attractive alternative to Cs frequency standards. Our ^{87}Rb fountain has already been described in detail in ref.[21]. In this section, we present measurements of the two main atom number dependent effects in a ^{87}Rb fountain, the collisional frequency shift and the cavity pulling effect.

As explained above, in a fountain the atoms interact twice with a microwave field (Ramsey method), inducing transitions between the two internal states $|g\rangle$ and $|e\rangle$. The collisional frequency shift is due to the interaction between atoms inside the atomic cloud during the Ramsey interaction. At very low temperatures, only s-wave scattering occurs and the collision between two atoms in internal states $|i\rangle$ and $|j\rangle$ is described using the scattering length $a_{i,j}$. Here, $|i\rangle$ and $|j\rangle$ refer to any atomic Zeeman substate $|F, m_F\rangle$, while $|g\rangle$ and $|e\rangle$ are notations for the clock levels only. In the case of ^{87}Rb, the lower and higher clock levels are $|g\rangle = |1,0\rangle$, and $|e\rangle = |2,0\rangle$. In the general case where states other than $|g\rangle$ and $|e\rangle$ are populated, the clock frequency shift is related to the partial densities n_j of states $|j\rangle$ by the following expression [20]:

$$\Delta\nu = -\frac{2\hbar}{m} \times \sum_j n_j (1+\delta_{g,j})(1+\delta_{e,j})(a_{g,j} - a_{e,j}) \quad (2)$$

where the Kronecker symbol $\delta_{i,j}$ accounts for quantum statistics. In a fountain, the partial densities n_j are space- and time-dependent and the measured frequency shifts appear as an average over these variables.

The second effect which depends on atom number is the cavity frequency pulling [22]. In our fountain, the atomic transition is probed by a 6.8 GHz microwave field in a TE_{011} copper resonator with a quality factor $Q \simeq 10^4$. The pulling effect is due to the interference inside the microwave resonator between the field radiated by the input coupler and the field radiated by the atomic magnetic dipoles when the atoms pass through the cavity. This interference induces a time dependent phase shift between the field inside the resonator and the signal delivered by the oscillator. It produces a clock shift that exhibits a dispersive dependence as a function of the cavity detuning with respect to the atomic resonance ($\Delta\nu_{\rm cav} = \nu_{\rm cav} - \nu_{\rm at}$). The amplitude of this dispersion curve is proportional to Q and to the number of atoms N_{cav} crossing the cavity. The width is proportional to $1/Q$. When the atoms enter the cavity in the upper state (resp. lower state) and deposit (resp. extract) energy in the cavity, the clock frequency is *pulled* towards (resp. *pushed* away from) the cavity resonance frequency.

Our treatment of the frequency shift measurements takes into account both collisional frequency shift and cavity pulling simultaneously. By tuning the cavity around the Rb resonance frequency, we display the caracteristic dispersive lineshape of the cavity pulling effect and find good agreement with theory (fig.4). A quantitative model of the pulling effect allows us to make a precise determination of the number of atoms crossing the cavity, N_{cav}. The measurements of the velocity distribution and of the initial size of the atomic cloud, combined with a Monte-Carlo simulation and the measurement of N_{cav}, give the average atomic density during the Ramsey interrogation ($\overline{n}$). After subtraction of the pulling contribution, we thus deduce the collisional frequency shift. In order to test the Monte-Carlo simulation, other methods have been used to measure the number of atoms in the fountain (experimental details are given in ref.[9]). These methods agree with the value deduced from the cavity pulling within 20%.

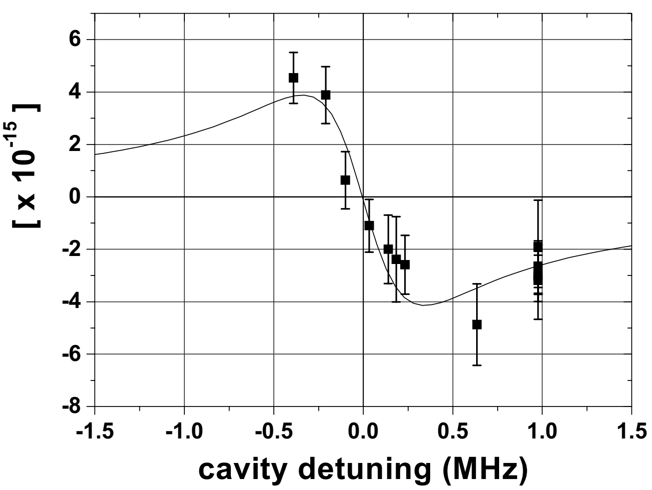

Figure 4: Relative frequency shift vs cavity detuning for $\Delta N = 3.5 \times 10^7$ in case (i). Solid line : fit from eq. (3).

Our measurement approach uses a differential method. Every 200 fountain cycles (~ 350 s), we change the trapping light intensity so that the number of atoms in the fountain alternates between two values $N_{\rm high}$ and $N_{\rm low} \simeq N_{\rm high}/4$. We measure the frequency difference between the two situations. This method efficiently rejects slow frequency fluctuations which are not related to atom number or density, in particular the H-maser drift. In the differential method the frequency resolution is $\sim 3 \times 10^{-13}\tau^{-1/2}$ where τ is the averaging time in seconds. At 350 s the maser stability is $\sim 2.7 \times 10^{-15}$, at least 4 times better than the fountain stability. The relative frequency resolution on effects which depend on atom number reaches $\sim 1 \times 10^{-15}$ per day.

After launch, atoms are spread among the various m_F substates of the $F = 2$ manifold. Data have been taken in three cases. (i) normal clock operation : atoms in the $|2,0\rangle$ substate are transferred to $|1,0\rangle$ using a microwave π pulse. Atoms remaining in $|2, m_F \neq 0\rangle$ are pushed away by radiation pressure. Only three scattering lengths a_{gg}, a_{ge} and a_{ee} in eq. (2) are involved. (ii) no selection : all Zeeman sublevels in $F = 2$ are equally populated to within $2-3\%$. The frequency shift of the $|2,0\rangle \rightarrow |1,0\rangle$ transition is measured in the presence of $|2, m_F \neq 0\rangle$ populations. (iii) Atoms are pumped in $F = 1$ by a laser pulse tuned to the $F = 2 \rightarrow F' = 2$ optical transition. Atoms remaining in $F = 2$ state ($\lesssim 2\%$) are pushed away by radiation pressure. The launched atoms are equally spread among the $F = 1$ substates to within 1%. The frequency shift of the $|1,0\rangle \rightarrow |2,0\rangle$ transition is measured in the presence of $|1, m_F \neq 0\rangle$ populations.

Fig. 4 shows the differential measurement of the clock frequency shift as a function of the cavity detuning $\Delta\nu_{\rm cav}$ with respect to the atomic resonance, for atoms initially selected in $|1,0\rangle$, with $N_{\rm high} \simeq 4.3 \times 10^7$ entering the microwave cavity and $N_{\rm low} \simeq 0.8 \times 10^7$. The simulation shows that this modulates the effective density by a factor ~ 3.3, because both velocity distribution and initial size of the atomic cloud depend on the regime of operation of the fountain (high or low number of atoms). The frequency and quality factor of the cavity are measured with an uncertainty of 20 kHz and 4% respectively and the cavity is tuned by temperature [23]. The solid line is a least square fit of the data using the following function :

$$\delta\nu/\nu = f(\Delta\nu_{cav})\Delta N + B\Delta\bar{n} \qquad (3)$$

where B is the free parameter of the fit, and $\Delta N = N_{\rm high} - N_{\rm low}$ [24]. $f(\Delta\nu_{\rm cav})$ is the calculated dispersive line shape of the cavity pulling effect for a single atom in the cavity. $\overline{n}$ is the effective atomic density and is related to the partial densities n_j in eq.(2) by $\overline{n} = \sum_j \overline{n}_j$, where $\overline{n}_j$ are the partial densities $n_j(t)$, averaged over time, over the initial spatial distribution and over the velocity distribution.

We find $B = -7.2(20.0) \times 10^{-24}\,\rm cm^3$. B, the collisional shift coefficient, is surprisingly consistent with zero even with a frequency standard deviation of 3×10^{-16} given by the fit. Thus in case (i), at a density of $1.5 \times 10^7\,\rm cm^{-3}$, ^{87}Rb exhibits no detectable shift (fig. 5(i)) whereas ^{133}Cs would exhibit a shift of 3×10^{-14}. Our upper value for the ^{87}Rb collisional shift is consistent with the recent measurement of C. Fertig and K. Gibble giving $-0.38(8)$ mHz for a density of $1.0(6) \times 10^9\,\rm cm^{-3}$ [8].

Fig. 5 summarizes the collisional shifts measurements versus the effective density $\bar{n}$ in the three cases (i), (ii) and (iii) [25]. By contrast to case (i), data recorded in case (ii) and (iii) show a clear dependence with the density after subtracting the cavity pulling effect.

The measured value in case (ii) $-50(10)(^{+22}_{-34}) \times 10^{-24}\,\rm cm^3$ is in reasonable agreement with the theoretical predictions $-56 \times 10^{-24}\,\rm cm^3$ [20] and $-33 \times 10^{-24}\,\rm cm^3$ [26]. The first parenthesis refers to the frequency statistical uncertainty (1 standard deviation); the second to the linear combination of frequency uncertainty and density calibration uncertainty. From variations of the parameters in the simulation and experimental calibrations , we deduce a 35% type B uncertainty on our density. Adding quadratically the 11% statistical uncertainty on atom number, we get a 40% combined uncertainty on the density. This corresponds to a scale factor of 1.4 and 1/1.4 on the density axis of fig. 5, defining the acceptance domain of the measurements (dotted lines). In case (iii), the agreement with theory is similar. We find $-60(16)(^{+29}_{-46}) \times 10^{-24}\,\rm cm^3$ to be compared to $-68 \times 10^{-24}\,\rm cm^3$(ref. [20]) and $-41 \times 10^{-24}\,\rm cm^3$ (ref. [26]). Finally, our data in case (i), $-7.2(20.0)(^{+25}_{-31}) \times 10^{-24}\,\rm cm^3$ show a disagreement at $\sim 3\sigma$ with theory of ref. [20] and seem to favor the more recent theory of ref. [26].

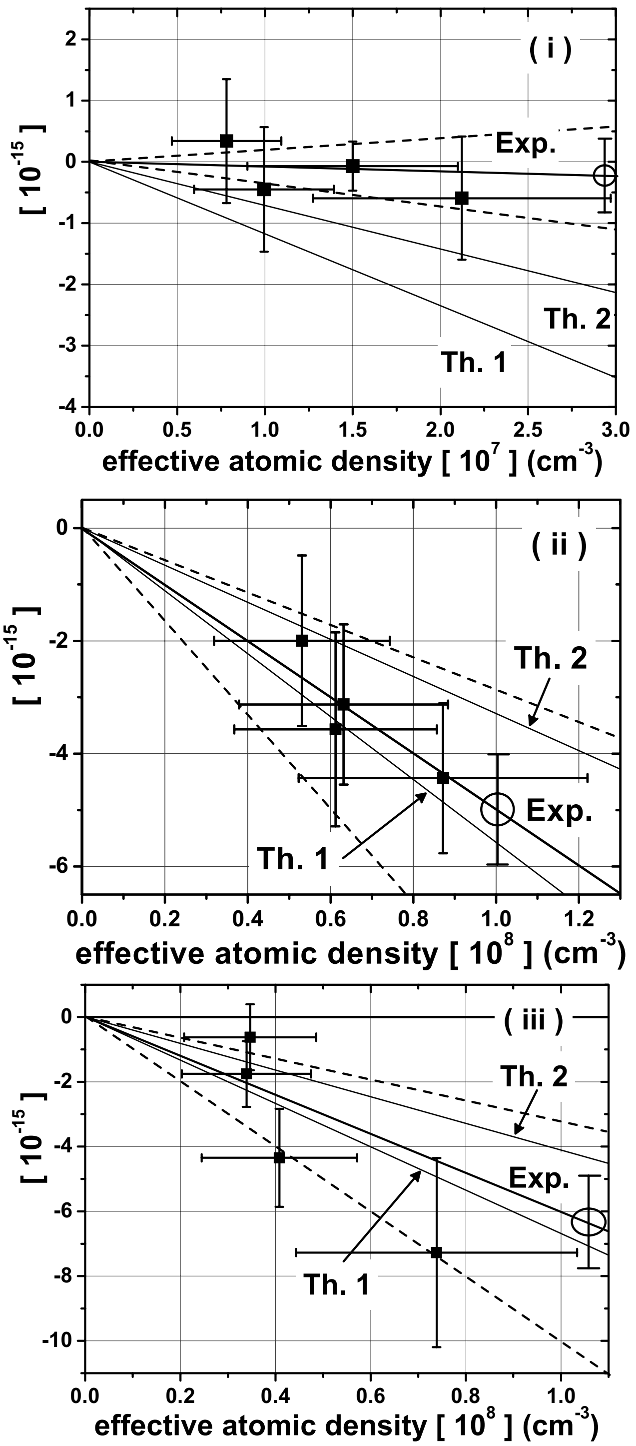

Figure 5: Frequency shift of the $|1,0\rangle \rightarrow |2,0\rangle$ transition vs effective density in cases (i),(ii), and (iii), and comparison with theories of ref. [20] (Th.1) and ref. [26] (Th.2). Open circles :linear fits to the experimental data with statistical frequency uncertainty at the given density. Horizontal error bars represent the 40% density uncertainty. Dotted lines : experiment with combined frequency and density uncertainties.

4 A NEW LIMIT FOR the VARIATION OF α WITH TIME

4.1 Present tests

Comparing the hyperfine energies of different alkali or alkali-like species provides an interesting test of the Local Position Invariance, which is one of the statements of the Einstein Equivalence Principle (EEP). *"In local freely falling frames, the outcome of any non-gravitational test experiment is independent of where and when it is performed"*. Experimental tests of the EEP thus aim at determining the relative rate of change of non-gravitational fundamental constants, such as the fine structure constant $\alpha = e^2/\hbar c$, either with time or with the gravitational potential. A variation of α would violate the EEP, and give support to recent many-dimensional cosmologies (Kaluza-Klein models, superstring theories) that attempt to unify gravity and other fundamental forces ([27, 28, 29]). Two types of tests of the stability of α are being performed : at the cosmological and at the laboratory scale. An example of cosmological measurement is the Oklo test. This test analyses the isotope ratios $^{149}Sm/^{147}Sm$ in the natural uranium fission reaction that took place around 1.8×10^9 years ago (corresponding to a redshift $z \approx 0.1$) at the present day site of the Oklo mine in Gabon, West Africa. Recent analysis of the Oklo data [30] has shown that:

$$-0.9 \times 10^{-7} \leq (\alpha_{Oklo} - \alpha_{now})/\alpha_{now} \leq 1.2 \times 10^{-7} \quad (4)$$

so that, integrating over 1.8×10^9 years, one obtains:

$$|\dot{\alpha}/\alpha| \leq 5 \times 10^{-17}\, yr^{-1} \quad (5)$$

In a similar way, astrophysical methods make it possible to estimate α at earlier evolutionary phases of the Universe and determine $|\dot{\alpha}/\alpha|$ as a function of redshift z (i.e. cosmological time), by making spectroscopic observations of gas clouds against background quasars. Extensive analysis has been carried out by various groups, measuring the relativistic fine-structure splitting of alkali-type resonance doublets. This method is based on the fact that the separation between lines within one multiplet is proportional to α^2. Measuring the doublet separation in an absorption system and comparing with laboratory values, one can estimate the difference between α at the epoch z and the present value. D. A. Varshalovich *et al.* [31] focused on the analysis of $SiIV$ doublets absorbed by 3 quasars located at $z \approx 3$, paying special attention to the non-linearities in the dispersion curves of the echelle spectrograph used for the observations. Their analysis leads to an upper bound, at the 2σ level:

$$|\Delta\alpha/\alpha| \leq 1.6 \times 10^{-4} \quad (6)$$

and, averaged over 10^{10} years,

$$|\dot{\alpha}/\alpha| \leq 1.6 \times 10^{-14}\, yr^{-1} \quad (7)$$

J.K. Webb *et al.* [32, 33] recently analysed $MgII$ and $FeII$ doublets absorption spectra emitted by 25 quasars, thus spanning a wide range of epochs ($0.6 < z < 1.6$). Their measurements display a clear departure from zero at the 3σ level, when considering the sample as a whole:

$$|\Delta\alpha/\alpha| = (-1.09 \pm 0.36) \times 10^{-5} \quad (8)$$

However, the $0.6 < z < 1.0$ points alone show no significant trend:

$$|\Delta\alpha/\alpha| = (-0.17 \pm 0.39) \times 10^{-5} \quad (9)$$

These results make the issue of the fine structure constant temporal variation particularly acute.

As noted in [34, 35], laboratory measurements based on clock comparisons contrast with cosmological measurements, because they are repeatable and span over monthly to yearly durations ($z \ll 1$). They thus provide complementary information to the cosmological determinations. These clock comparisons involve ultrastable oscillators of different compositions such as superconducting cavities vs H-maser or Cs hyperfine structure transition (case (i)) [34], or atomic clocks with different species (case (ii)): Mg fine structure transition vs Cs hyperfine transition [36], Hg^+ ion frequency standard vs H-maser [35]. In case (i), tests rely on the fact that the cavity frequency is proportional to α while the H-maser or Cs clock transition is proportional to α^2 (at first order). In case (ii), the method is based on the increasing importance of Casimir relativistic contribution to the hyperfine energy splitting as atomic number Z inceases in the group I alkali elements and alkali-like ions [35, 37]. A temporal variation of the ratio of the hyperfine energies of different alkali would thus provide a signature of the temporal variation of α. Prestage *et al.* [35] derived an upper bound for $|\dot{\alpha}/\alpha|$ from the comparison of Hg^+ vs H-maser:

$$\frac{d}{dt}\ln(\frac{\nu_{Hg^+}}{\nu_H}) = +2.2 \times |\dot{\alpha}/\alpha| \quad (10)$$

and:

$$|\dot{\alpha}/\alpha| \leq 3.7 \times 10^{-14}\, yr^{-1} \quad (11)$$

4.2 Comparisons between ^{87}Rb and ^{133}Cs fountains

With our two Cs fountains and one Rb fountain in operation, we can compare Cs and Rb hyperfine frequencies in time, and search for a possible temporal variation of α. Since 1998, three campaigns of measurements of the ^{87}Rb absolute frequency have been performed with reference to the Cs fountain. During each campaign, several parameters such as the launch height of the atomic cloud in the fountain, the microwave power, and the magnetic field have been varied. The accuracy budget of the Rb fountain was thus re-evaluated each time. Each frequency measurement was corrected for systematic shifts. The obtained values were then binned, giving one frequency data point for each campaign. In fig. 6, we have plotted the relative frequency shift $(\frac{\Delta\nu}{\nu})_{Rb}$, where $(\Delta\nu)_{Rb} = (\nu(t) - \nu(t_0)$, versus time. Here, $\nu(t)$ accounts for the frequency measurement at time t. t_0 corresponds arbitrarily to our second campaign (April 1999). A linear fit to the data points over two years leads to :

$$\frac{d}{dt}\ln(\frac{\nu_{Rb}}{\nu_{Cs}}) = (1.9 \pm 3.1) \times 10^{-15}\, yr^{-1} \tag{12}$$

The 3.1×10^{-15} uncertainty is the quadratic sum of the accuracy of the Rb fountain (1.4×10^{-15}), the accuracy of the Cs fountain (1.1×10^{-15}), and of the statistical noise in the frequency comparison(2.5×10^{-15}). This uncertainty of 3.1×10^{-15} represents a 20-fold improvement in the accuracy of long term clock frequency comparisons over previous work [35].

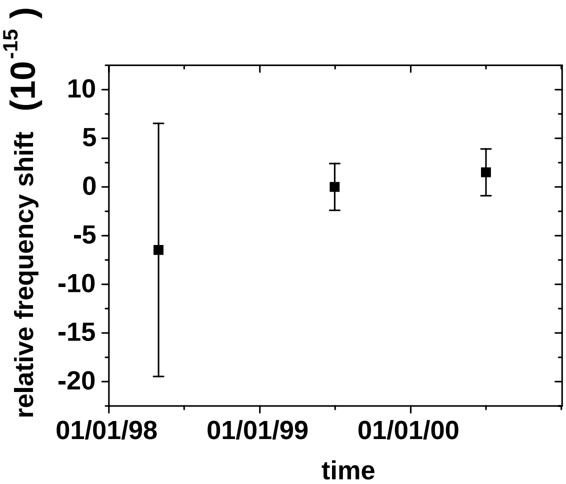

Figure 6: Measured ^{8}7Rb frequencies referenced to the ^{133}Cs fountain FO1. The measurement in April 1999 is 6834682610.904343 Hz. The errors bars represent the combined inaccuracies of ^{87}Rb and ^{133}Cs fountains.

In the interpretation of these results, we first assume, as in [35], that there is no time dependence of the ^{133}Cs and ^{87}Rb nuclear magnetic moments. Then, all possible drift of the hyperfine energy ratio ν_{Rb}/ν_{Cs} can be attributed to the Casimir relativistic correction $F_{rel}(\alpha Z)$. Under this assumption, we obtain :

$$|\dot{\alpha}/\alpha| = (4.2 \pm 6.9) \times 10^{-15}\, yr^{-1} \tag{13}$$

an improvement by a factor 5 over the previous H-maser-Hg^{+} comparison [35]. Conversely, as pointed out by S. Karshenboim [37], our measurements can also set an upper limit to the time variation of the proton magnetic moment g_p, if we now assume no time variation of α. This test is then 4 times more sensitive than the test over α, and we find :

$$|\frac{\dot{g_p}}{g_p}| = (9.5 \pm 16) \times 10^{-16}\, yr^{-1} \tag{14}$$

Of course any combination of these two extreme assumptions is possible and more tests with different alkali and alkali-like atoms will severely constrain these limits in the future.

5 ACES : atomic Clock Ensemble in Space

ACES is a space mission which has been selected by the European Space Agency (ESA) to fly on the international space station (ISS) in 2004 [38]. ACES consists of two clocks, a cold atom clock (PHARAO) and a hydrogen maser (SHM, Neuchâtel Observatory), together with microwave and optical links for time and frequency transfer to ground users. These equipments will fit on a nadir oriented express pallet of dimensions $863 \times 1168 \times 1240$ mm. The total mass will not exceed 225 kg and the electrical power 500 Watts (fig.7).

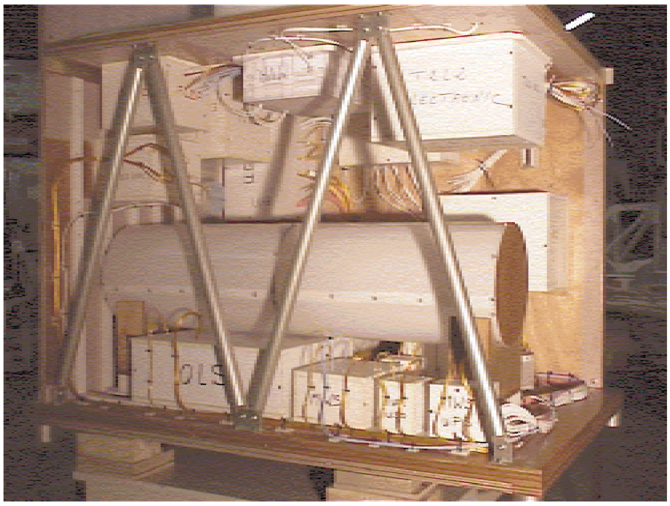

Figure 7: Mock-up of the ACES plattform

Because micro-gravity allows long interaction times between the atoms and the microwave field and because the atomic velocity is smaller than in earth fountains and constant, we expect an excellent accuracy for a cold atom space clock [10, 11, 39]. The specified frequency stability of PHARAO for ACES is better than $1\ 10^{-13}\tau^{-1/2}$. Averaged over one day, this stability should be $3\ 10^{-16}$. Its projected accuracy is $1\ 10^{-16}$.

Scientific objectives of ACES also include measurement of the gravitational red-shift with a 25-fold improvement over the Gravity Probe A mission of Vessot *et al.* [40], a better test of the isotropy of speed of light and a search for a possible drift of the fine structure constant α. Finally, with the time transfer equipments, ACES will allow synchronization of time scales of distant ground laboratories with 30 ps accuracy and frequency comparisons with 10^{-16} accuracy. Similar space clock projects are also under development in the USA, PARCS [41] and RACE [42].

6 Prospects

Microwave frequency standards using fountains are now in their maturity; a frequency stability of 6 10^{-16} has been measured and the present accuracy is 1 10^{-15}. Operating permanently with an SCO as interrogation oscillator, the fountain frequency stability should enter into the low 10^{-16} range in the reasonable averaging time of one day. The two dominant terms in the present accuracy budget are the blackbody radiation shift and the collisional shift. The latter prevents the use of large number of atoms, unless more complicated techniques such as juggling or cw fountains are used. Calculations show that the cavity phase shift is negligible at the 10^{-15} level, but it must be carefully evaluated when asking for a one order of magnitude gain. Rb fountains, because of the strongly reduced collisional shift are likely to push the accuracy further, i.e. in the 10^{-17} range. Fountains now operate at the fundamental quantum limit for uncorrelated particles. An attractive line of research is to apply the recently proposed spin squeezing techniques to improve the frequency stability beyond the projection noise limit proportional to $1/\sqrt{N_{at}}$ [43, 44, 45]. A factor of $1/\sqrt{N_{at}}$ can ultimately be gained.

With their relative simplicity, fountain devices compete favorably with laser cooled trapped ion frequency standards. However, practically unlimited interaction times can be achieved with trapped charged particles. This is an advantage for increasing the quality factor. On the other hand, ions interact much more by Coulomb repulsion than neutrals and traps with a single ion (or a small number) must be used [2]. This is then made at the expense of signal to noise ratio hence of short term stability, even if quantum limited detection is implemented using the quantum jump method.

Microwave cold atom standards ultimately will be limited by the quality factor of the atomic line. Very narrow transitions in the optical domain offer attractive possibilities for fountains with neutrals [46]. A prominent example is the $1s-2s$ transition of hydrogen [47, 48, 49], measured recently with a frequency resolution of 1.8 10^{-14} by comparison with the PHARAO transportable fountain [3]. Alkali-earth atoms are good candidates since they have already been laser cooled and possess forbidden transitions in the visible domain. Progress with laser cooled Ca, Mg and Sr using intercombination lines has been spectacular [4, 50, 51, 52, 53]. All these frequency standards, with ions or neutrals, require ultra-stable laser sources to interrogate these narrow lines and a recent breakthrough has been made by the NIST Boulder group measuring sub-Hertz laser linewidth in the visible range [54]. In addition, the recent progress on frequency combs using femtosecond lasers opens new possibilities for comparing microwave and optical frequency standards at 10^{-16} or below [55, 49, 56].

These atomic frequency standards can already be compared at 1 10^{-15} using the transportable PHARAO device. Frequency comparisons of distant clocks using satellite time transfer, GPS-phase or two way techniques, are presently at the level of $\sim$ 3 10^{-15} for an averaging time of 2 10^4 s [57] and $\sim$ 2 10^{-15} for one day [58]. Global comparisons between fountains will improve the quality of the TAI (Temps Atomique International). In fine, these high performance frequency standards will allow new tests in fundamental physics as well as new applications in navigation, positioning and geodesy.

We acknowledge fruitful discussions with Y. Castin, C. Cohen-Tannoudji, J. Dalibard, G. Shlyapnikov and the ENS group. We are thankful to A. Gérard, M. Lours, M. Dequin, L. Volodimer, P. Petit and to the SERT for technical support. Work supported in part by BNM and CNRS. BNM-LPTF and Laboratoire Kastler Brossel are Unités Associées au CNRS, UMR 8630 and UMR 8552.

References

[1] Galluzzi P., this volume

[2] Berkeland D., Miller J., Bergquist J., Itano W., and Wineland D., *Phys. Rev. Lett.*, **80**, 2089 (1998).

[3] Niering M. *et al.*, *Phys. Rev. Lett.*, **84**, 5496 (2000).

[4] Riehle F. *et al.*, *IEEE Trans. Inst. Meas.*, **48**, 608 (1999).

[5] Kasevich M., Riis E., Chu S. and de Voe R., *Phys. Rev. Lett.*, **63**, 612 (1989).

[6] Clairon A., Salomon C., Guellati S., and Phillips W., *Europhys. Lett.*, **16**, 165 (1991).

[7] Santarelli G. *et al.*, *Phys. Rev. Lett.*, **82(23)**, 4619 (1999).

[8] Fertig C. and Gibble K., *Phys. Rev. Lett.*, **85**, 1622 (2000).

[9] Sortais Y. *et al.*, *Phys. Rev. Lett.* in press, scheduled 09 oct. 2000.

[10] Clairon A. *et al.*, in *Proc. of the* 6^{th} *European Frequency and Time Forum*, ESA : **SP-340**, pp. 27–33 (1992).

[11] Lounis B., Reichel J., and Salomon C., *C.R. Acad. Sci. (Paris)*, **316(2)**, 739 (1993).

[12] Santarelli G.*et al.*, *IEEE Trans. Ultr. Ferr. Freq. Contr.*, **45**, 887 (1998).

[13] Luiten A., Mann A., Costa M., and Blair D., *IEEE Trans. Instr. Meas.*, **44**, 132 (1995).

[14] Wineland D., Itano W., Bergquist J., and Walls F., in *Proc.* 35^{th} *Ann. Freq. Contr. Symp.* (1981).

[15] Itano W. *et al.*, *Phys. Rev. A.*, **47**, 3554 (1993).

[16] Dick G., in *Proc. of Precise Time and Time Interval*, pp. 133–147, Redendo Beach (1987).

[17] Tjolker R., Prestage J., and Maleki L., in J. Bergquist ed., *Proc. of* 5^{th} *Symp. on Freq. Stand. and Metr.*, World Scientific, Singapore (1996).

[18] Fisk P., Sellars M., Lawn M., and Coles C., *ibid.*

[19] Clairon A. *et al.*, *IEEE Trans. on Inst. and Meas.*, **44(2)**, 128 (1995).

[20] Kokkelmans B., Verhaar B., Gibble K., and Heinzen D., *Phys. Rev. A.*, **56**, R4389 (1997).

[21] Bize S. *et al.*, *Europhys. Lett.*, **45(5)**,558 1999.

[22] Vanier J. and Audoin C., *The Quantum Physics of Atomic Frequency Standards*, Bristol and Philadelphia : Adam Hilger, 1989.

[23] Fertig C. and Gibble K., *IEEE. Trans. Instrum. Meas.*, **48**, 520–523 (1999).

[24] In fig.(1) we have rescaled the data to a fixed $\Delta N = 3.5 \times 10^7$. During the 6 month data acquisition, ΔN typically fluctuated by 20%.

[25] To clarify fig.(5i), we represent, in place of individual measurements, the weighted average of 10 of them performed at very similar densities ($1.5(2)\ 10^7\ \mathrm{cm}^{-3}$).

[26] Williams C. *et al.*, private communication.

[27] Damour T. and Polyakov A., *Nucl. Phys.*, B**423**, 532 (1994).

[28] Wu Y. and Wang Z., *Phys. Rev. Lett.*, **57**, 1978 (1986).

[29] Marciano W., *Phys. Rev. Lett.*, **52**, 489 (1984).

[30] Damour T. and Dyson F., *Nucl. Phys.*, B**480**, 37 (1996).

[31] Varshalovich D., Panchuk V., and Ivanchik A., *Astr. Lett.*, **22**, 6 (1996).

[32] Webb J., Flambaum V., Churchill C., Drinkwater M., and Barrow J., *Phys. Rev. Lett.*, **82(5)**, 884 (1999).

[33] Flambaum V. *et al.*, this volume.

[34] Turneaure J., Will C., Farrel B., Mattison E., and Vessot R., *Phys. Rev. D*, **27**, 1705 (1983).

[35] Prestage J., Tjoelker R., and Maleki L., *Phys. Rev. Lett.*, **74**, 3511 (1995).

[36] Godone A., Novero C., Tavella P., and Rahimullah K., *Phys. Rev. Lett.*, **71**, 2364 (1993).

[37] Karshenboim S., this volume and submitted to *Can. Journ. of Physics.*

[38] Salomon C. and Veillet C., in *Proc. on "Space Station Utilisation"*, ESA Symposium, **SP-385**, 295 (1996).

[39] Laurent P. *et al.*, *Euro. Phys. J. D*, **3**, 201 (1998).

[40] Vessot R. *et al.*, *Phys. Rev. Lett.*, **45**, 2081 (1980)

[41] Robinson H. *et al.*, in *Proc. of IEEE Int. Freq. Contr. Symp.*, pp. 37–40 (1998)

[42] Gibble K., *ibid.*, pp. 41–45.

[43] Wineland D., Bollinger J., Itano W., Moore F., and Heinzen D., *Phys. Rev. A*, **46**, 6797 (1992).

[44] Kuzmich A., Mölmer K., and Polzik E., *Phys. Rev. Lett.*, **79**, 4782 (1997).

[45] Sorensen J., Hald J., and Polzik E., *Phys. Rev. Lett.*, **80**, 3487 (1998).

[46] Hall J. and Zhu M., *Journ. Opt. Soc. A. B*, **6**, 2194 (1989).

[47] Beausoleil G. and Hänsch T., *Phys. Rev. A*, **33**, 1661 (1986).

[48] Udem T. *et al.*, *Phys. Rev. Lett.*, **79**, 2646 (1997).

[49] Udem T. *et al.*, in *Proc. of the Opt. Freq. Synth. and Metr. Symp.*, Springer Verlag (2000).

[50] Hollberg L. *et al.*, *ibid.*

[51] Ruschewitz F. *et al.*, *Phys. Rev. Lett.*, **80**, 3173 (1998).

[52] Vogel K. , Dinneen T., Gallagher A., and Hall J., *IEEE Trans. Inst. Meas.*, **48**, 618 (1999).

[53] Katori H., Ido T., Isoya Y., and Kuwata-Gonokami M., *Phys. Rev. Lett.*, **82**, 1116 (1999).

[54] Young B., Cruz F., Itano W., and Bergquist J., *Phys. Rev. Lett.*, **82**, 3799 (1999).

[55] Diddams S. *et al.*, *Phys. Rev. Lett.*, **84(22)**, 5102 (2000).

[56] Luiten A. *et al.*, in *Proc. of the Opt. Freq. Synth. and Metr. Symp.*, Springer Verlag (2000).

[57] Petit G., Thomas C., Jiang Z., Uhrich P., and Taris F., *IEEE Trans. Ultr. Ferr. Freq. Contr.*, **46**, 941 (1999).

[58] Larson K. and Levine J., in *Proc. of IEEE Int. Contr. Symp.*, p. 292 (1998).